Journal of Alloys and Compounds 522 (2012) 3–8

Contents lists available at SciVerse ScienceDirect

Journal of Alloys and Compounds

journal homepage: www.elsevier.com/locate/jallcom

Disk-type piezoelectric transformer of a $Na_{0.5}K_{0.5}NbO_3$–$CuNb_2O_6$ lead-free ceramic for driving T5 fluorescent lamp

Ming-Ru Yang [a,b], Sheng-Yuan Chu [a,c,*], I.-Hao Chan [d], Song-Ling Yang [a]

[a] Department of Electrical Engineering, National Cheng Kung University, Tainan 701, Taiwan
[b] Green Energy and Environment Research Laboratories, Industrial Technology Research Institute, Hsinchu 310, Taiwan
[c] Advanced Optoelectronic Technology Center, National Cheng Kung University, Tainan 701, Taiwan
[d] Institute of Microelectronics, Department of Electrical Engineering, National Cheng Kung University, Tainan 701, Taiwan

ARTICLE INFO

Article history:
Received 3 September 2010
Received in revised form 18 October 2011
Accepted 19 October 2011
Available online 18 November 2011

Keywords:
NKN
Ceramic
Lead-free
Piezoelectric
Transformer

ABSTRACT

Lead-free $(Na_{0.5}K_{0.5})NbO_3$ (NKN) ceramics doped with 1 mol% $CuNb_2O_6$ (CN) ceramics were prepared using the conventional mixed oxide method, with a sintering temperature of 1075 °C. Microstructural analyses of the NKN–01CN ceramics were carried out and compared, using X-ray diffraction (XRD). NKN–01CN ceramics sintered at 1075 °C not only exhibited excellent 'hard' piezoelectric properties of k_p = 40%, k_t = 45%, k_{33} = 57%, a ferroelectric property of E_c = 23 kV/cm, and an extraordinarily high mechanical quality factor (Q_m) of 1933 but also showed excellent stability with temperature (TCF = −154 ppm/°C). The piezoelectric transformer was simplified, using an equivalent circuit, and analyzed, using MATLAB; the simulation data agreed well with the experimental results. An efficiency of 95.7% was achieved for the NKN–01CN piezoelectric transformer with load resistance of 20 kΩ. An 8 W T5 fluorescent lamp was successfully driven by the NKN–01CN piezoelectric transformer.

1. Introduction

Piezoelectric transformer (PT), which combines piezoelectric actuators and piezoelectric transducers, are good substitutes for traditional magnetic transformers. Piezoelectric transformers have many advantages, including their high voltage gain, high power density, high electromechanical efficiency and small size. Since the invention of the first PT was invented by Rosen [1], various types of PT have been developed, such as the disk-type, ring-type and multilayer [2–4]. Recently, piezoelectric transformers have been used in many applications, such as AC/DC converters, electronic ballasts for fluorescent lamps and inverters for driving CCFL (LCD backlights) [5,6].

Lead zirconate titanate (PZT) and PZT-based multi-component piezoelectric ceramics with a perovskite structure have been widely used in actuators, sensors, resonators, transducers and transformers because of their excellent piezoelectric and electrical properties [7,8]. However, the high volatilization of PbO, a main component of PZT ceramics, limits the use of these materials, because it contaminates the environment and harms human health, due to its toxicity. Lead-free materials have attracted increasing attention, as replacements for PZT-based piezoelectric ceramics. Sodium potassium niobate ($(Na_{0.5}K_{0.5})NbO_3$, NKN) ceramic is considered to be a good candidate for lead-free piezoelectric ceramics because of its strong piezoelectricity and ferroelectricity [9]. However, it is very difficult to synthesize ceramics with a dense microstructure, so many researchers have reported the addition of (Li, Sb, Ta) compounds to NKN ceramics, to improve the densification and enhance the piezoelectric properties of the samples [10–15]. In addition, CuO, or CuO compounds serve as good dopants for enhancing the Q_m value of NKN ceramics because of the formation of oxygen vacancies. A high Q_m is required for actuator and high-power applications, such as PT. Therefore, the microstructure, crystal and electrical properties of NKN ceramics, with CuO or CuO compounds have been widely investigated [16–20].

In this work, a small amount of Cu compound ($CuNb_2O_6$, CN) was selected as a dopant for NKN ceramics, to replace CuO. The results show that the CN-doped NKN specimens sintered at 1075 °C, display excellent 'hard' piezoelectric properties and ferroelectric properties. The mechanical quality factor (Q_m) of NKN ceramics with CN additive is extraordinarily high. CN improves the ability to be sintered and the electrical properties of NKN ceramics. The addition of a small amount of CN improves both the ability to be sintered and Q_m of NKN ceramics.

2. Experimental procedure

In a previous study [21], the authors found that $Na_{0.5}K_{0.5}NbO_3$ ceramics doped with 1 mol% $CuNb_2O_6$ have excellent piezoelectric properties. The samples of

* Corresponding author at: Department of Electrical Engineering, National Cheng Kung University, Tainan 701, Taiwan. Tel.: +886 6 2757575x62381; fax: +886 6 2345482.
E-mail address: chusy@mail.ncku.edu.tw (S.-Y. Chu).

0925-8388/$ – see front matter © 2011 Elsevier B.V. All rights reserved.
doi:10.1016/j.jallcom.2011.10.062

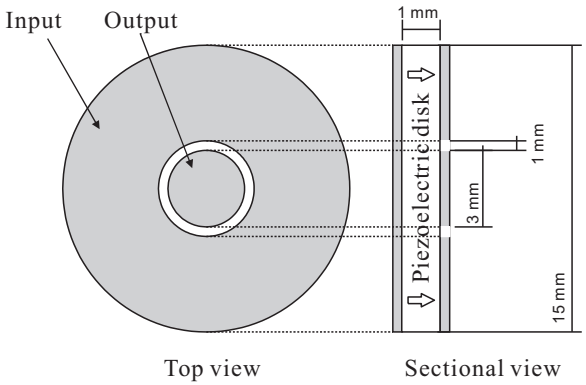

Fig. 1. Structure of a disk-type piezoelectric transformer.

starting materials of $Na_{0.5}K_{0.5}NbO_3$–$xCuNb_2O_6$ (NKN–xCN, for $x = 0$, and 1 mol%) processed using a conventional mixed-oxide method were pure reagent-grade Na_2CO_3 (SHOWA, 99.5%), K_2CO_3 (SHOWA, 99.5%), Nb_2O_5 (SHOWA, 99.5%) and CuO (SHOWA, 99.5%) powders. $Na_{0.5}K_{0.5}NbO_3$ (NKN) and $CuNb_2O_6$ (CN) were weighed in the desired compositions, respectively. The starting materials were individually transferred to a 100-mm-diameter cylindrical plastic jar, partially filled with 10 mm diameter ZrO_2 grinding balls. Sufficient ethanol (99.5%) was added to cover the powders. Ball milling was performed for 24 h, followed by drying at 130 °C, and then grinding, using an alumina mortar and pestle, to break up large agglomerates formed during drying. The stoichiometric NKN and CN powders were first synthesized, using a solid-state reaction method, at 850 °C, for 5 h and 900 °C, for 5 h, respectively. After the calcination, NKN and CN powders were weighed according to the formula of NKN–xCN and ball milled for 24 h. These powders, milled with 5 wt.% PVA aqueous solution, were uni-axially pressed into a disk of 18-mm diameter, at a pressure of 25 kg/cm^2 and subsequently sintered in air at 1075 °C, for 3 h.

Bulk densities were measured using the Archimedes method, with distilled water as the medium. The microstructure was observed using field emission scanning electron microscopy (FESEM), with a Hitachi S-4100 microscope. The crystallographic study was confirmed by X-ray diffraction (XRD) using Cu K_α ($\lambda = 0.154$ nm) radiation with a Siemens D-5000 diffractometer, operated at 40 kV and 40 mA. The dielectric and piezoelectric properties were measured with an HP 4294A precision impedance analyzer. To measure the electrical properties, silver paste was painted on both sides of the samples, to form electrodes; the samples were subsequently fired at 150 °C, for 20 min. Then, the samples were poled, in silicone oil, in a 30 kV/cm DC field at 150 °C for 30 min. The electromechanical coupling factor of thickness (k_t) and planar (k_p) mode was calculated using the resonance–antiresonance method. The piezoelectric coefficient, d_{33}, was measured using a Wide-Range d_{33} Tester 90-2030 (APC International, Ltd.). The coercive electric field (E_c) and the remnant polarization (P_r) were obtained in a 50 kV/cm 60 Hz AC field, using a modified Sawyer–Tower circuit [22]. In order to prevent arcing, the samples were submerged in 150 °C silicon oil.

In this experiment, an NKN–01CN piezoelectric disk of a 15-mm outer diameter, a 3-mm inner diameter and a 1-mm thickness was designed and evaluated as a disk-shaped PT. As shown in Fig. 1, the piezoelectric disk has silver electrodes. The width of the gap circle is 1-mm and the poling direction is the thickness direction. The characteristics of the transformer, under a variable load resistance, were investigated using the experiment setup shown in Fig. 2. The transformer was driven by a MOTECH FG-708S function generator and an NF BA4825 high speed bipolar amplifier. The voltage, current and power, at the input and output, were measured using a Tektronix TCP A300 current probe and a DPO 2024 digital phosphor oscilloscope.

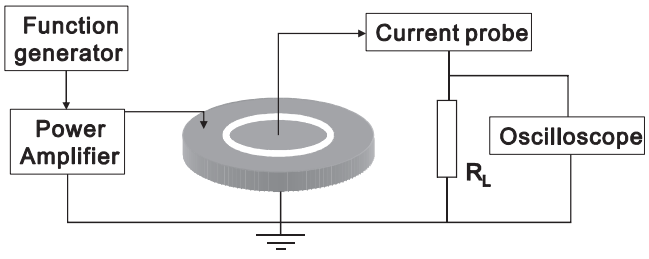

Fig. 2. Experimental setup for measurement of the characteristics of the piezoelectric transformer.

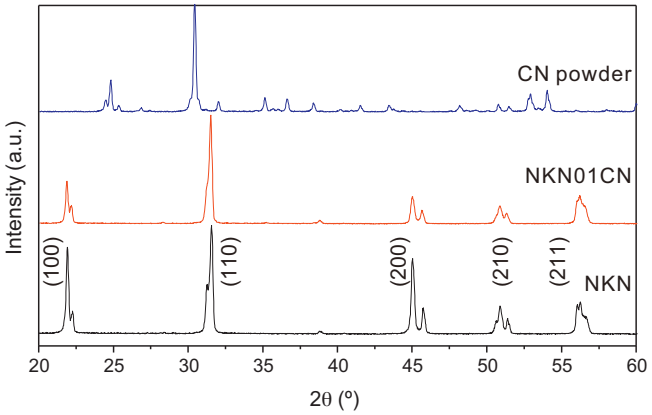

Fig. 3. XRD patterns of the CN powder, NKN–01CN ceramics, and NKN ceramics sintered at 1075 °C, for 3 h.

3. Results and discussion

The XRD patterns of the CN-modified NKN piezoelectric ceramics, sintered at 1075 °C, and CN powder are shown in Fig. 3. A homogeneous, pure NKN phase was well developed for 1 mol% CN additive. The main identified phase matches orthorhombic NKN with space group Amm2, at room temperature [23]. The results reveal that the orthorhombic perovskite structure is preserved (JCPDS card No. 32-0822). None of the phases ascribed to $CuNb_2O_6$ were detected. Fig. 4 shows the SEM images of NKN and NKN–01CN ceramics, sintered at 1075 °C. Both of the ceramics have a dense structure and the grains are generally rectangular in shape. For the NKN ceramic, the grains arrange in size from 1 to 2 μm. After

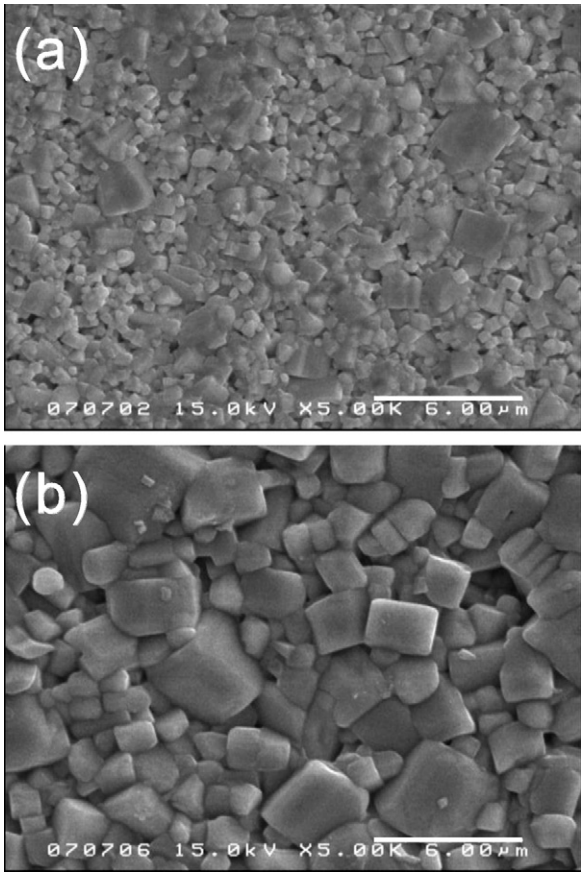

Fig. 4. SEM images of (a) NKN and (b) NKN–01CN ceramics, sintered at 1075 °C.

Table 1
Comparison of the properties of pure NKN and NKN–01CN ceramics.

	NKN	NKN–01CN
Density, ρ (g/cm^3)	4.08	4.47
Relative density (%)	91	99
Dielectric constant, ε_r	457	432
Poisson ratio, σ	0.26	0.25
k_p (%)	36	40
k_t (%)	37	45
k_{33} (%)	50	57
d_{33} (pC/N)	80	93
Q_m	227	1933
E_c (kV/cm)	9	26
P_r (μC/cm^2)	13.6	22.6
T_C (°C)	421	410
T_{O-T} (°C)	211	198

the doping of CN, the grains are obviously larger and the ceramic becomes denser. The abnormal grain growth usually occurs in the presence of the liquid phase and it may happen because of the low melting point of $K_4CuNb_8O_{23}$ (1050 °C). Because of the formation of a liquid phase, the sintering temperature for NKN ceramics is reduced and the densification is improved [21]. Meanwhile, the denser structure of NKN–01CN enhances the piezoelectric properties.

The material parameters of the NKN and NKN–01CN ceramics are summarized in Table 1. The density of NKN–01CN ceramics (4.47 g/cm^3) is much higher than that of NKN ceramics (4.08 g/cm^3). It is important that a piezoelectric transformer has a high electromechanical coupling factor (k_p) and mechanical quality factor (Q_m). In Table 1, the experimental results show that the k_p and Q_m values of pure NKN ceramics are 36% and 227, increasing to 40% and 1933, respectively, with the addition of 1 mol% CN. Pure NKN ceramics exhibit the typical features of 'soft' piezoelectric ceramics, whereas NKN–01CN exhibits 'hard' piezoelectric properties. The strong 'hardening' of the electrical properties can be attributed to the acceptor-doping effects of Cu ions. Therefore, Cu-substitution gives NKN 'hard' piezoelectric characteristics [19,20,24]. In the case of PZT, the addition of acceptor ions, such as Mg^{2+}, Sc^{3+}, and Fe^{3+}, increases the density of oxygen vacancies; this enhances the value Q_m. Cu^{2+} is considered to be a substitute for Nb^{5+} and behaves as an acceptor [19]. On the other hand, with the addition of CN, Cu^{2+} and Nb^{5+} may increase B site ions. A lower A/B ratio might increase the number of the oxygen vacancies and reduce the resonance impedance. Therefore, both Cu ion addition and excess B site ions are improve Q_m. A higher A/B ratio and the excess of the B site ions ($A/B < 1$) improve the mechanical quality factor (Q_m), electromechanical coupling factor (k_p) and the ability to be sintered [27,28]. Moreover, the Q_m value of all NKN–01CN ceramics is much higher than that of pure NKN ceramics.

In piezoceramic-based resonant devices, such as transducers, resonators and oscillators, the temperature coefficient of frequency (TCF) parameter is so important that it is usually used as a key index to evaluate the quality of these devices. To measure the values of TCF, samples were placed in a temperature-controlled furnace at temperatures from 0 °C (T_1) to 80 °C (T_2). The TCF values were calculated using:

$$TCF = \frac{f_{rT_2} - f_{rT_1}}{f_{rT_1} \times (T_2 - T_1)} \quad (1)$$

Fig. 5(a) shows the dependence of temperature on the rate of change of the resonant frequency (f_r) of pure NKN and NKN–01CN ceramics. As the temperature increases, from 0 °C to 80 °C, the rate of change of the resonant frequency of NKN–01CN ceramics becomes lower than that for NKN ceramics. When the temperature reaches 80 °C, the rate of change of the resonant

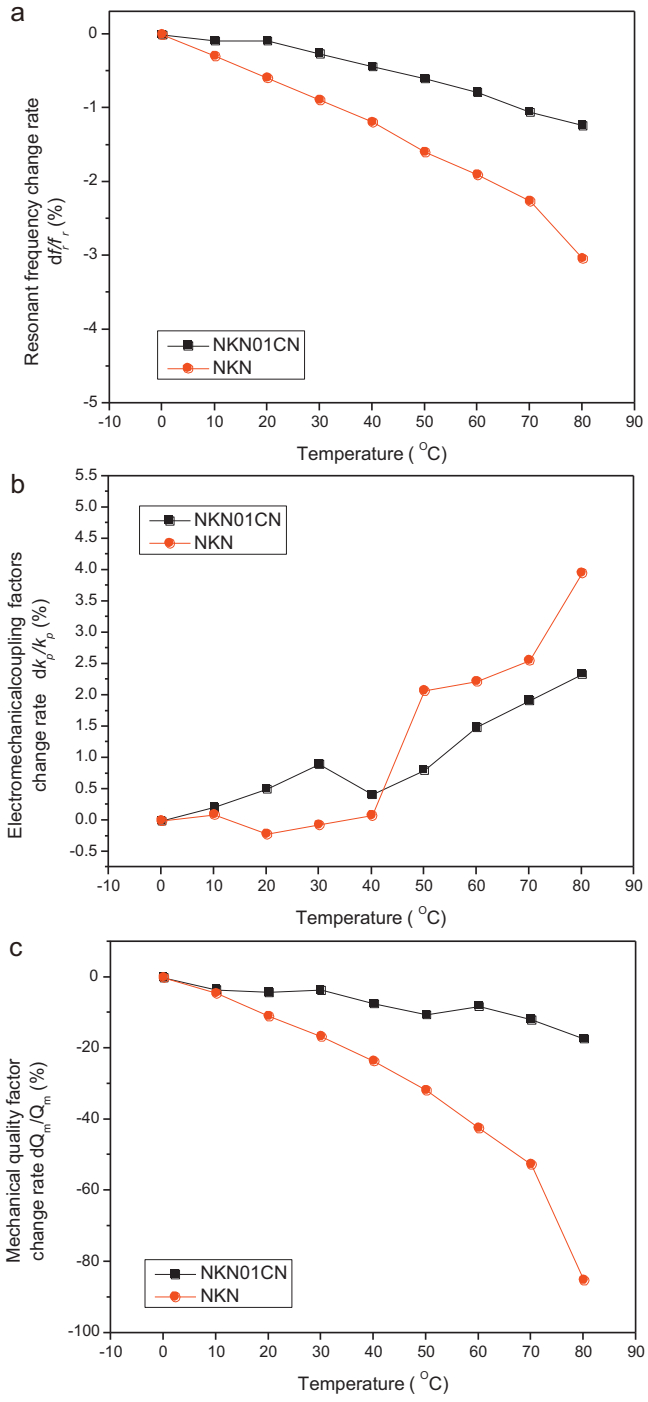

Fig. 5. Rate of change of (a) resonant frequency (f_r), (b) electromechanical coupling factor (k_p) and (c) mechanical quality factor (Q_m), for various temperatures.

frequency is calculated as −1.23% for NKN–01CN ceramics and −2.94% for pure NKN ceramics; the TCF values of NKN–01CN and NKN ceramics are −154 ppm/°C and −368 ppm/°C, respectively. Fig. 5(b) and (c) shows the rate of change of the values of Q_m and k_p, with temperature, from 0 °C to 80 °C. The rate of change of the characteristics of NKN–01CN ceramics are lower than those of NKN ceramics and in this temperature range, NKN ceramics with CN are much more stable than pure NKN ceramics.

Piezoelectric transformers, comparing pure NKN and NKN–01CN ceramics, were produced. Only the NKN–01CN transformer is discussed, because the impedance of the pure NKN

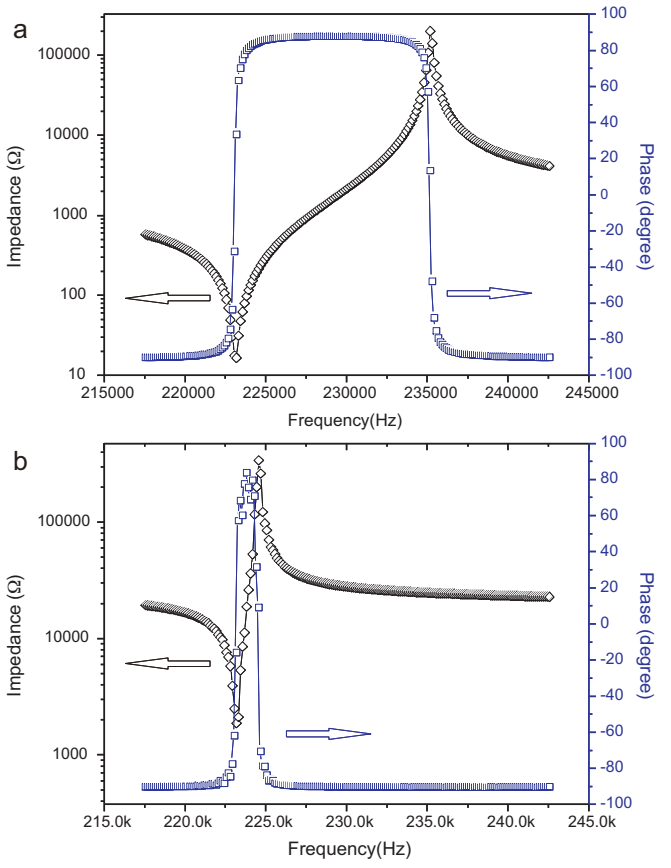

Fig. 6. Impedance of the NKN–01CN PT at the first vibration mode resonance: (a) the input with the output short-circuited and (b) the output with the input short-circuited.

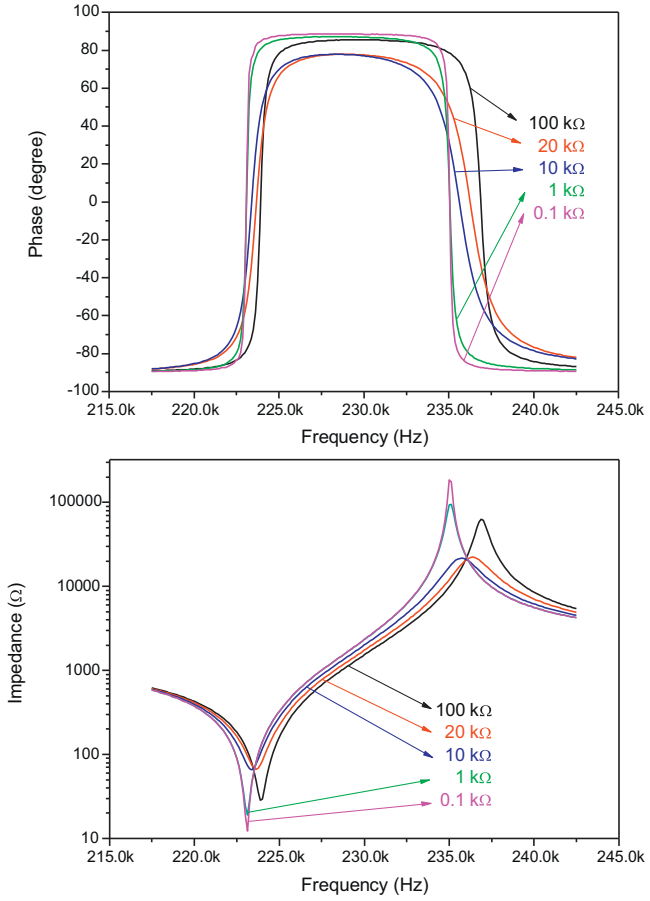

Fig. 7. Input impedance at various load resistances.

PT was too large and the current was too small to be measured, when an AC voltage was applied. The impedances of the NKN–01CN PT are shown in Fig. 6. The input impedance was measured with the output short-circuited and the output impedance was measured with the input short-circuited. The transformer operated in the first vibration mode. The first resonant frequencies (f_r) of the input and output are the same (223 kHz), but the anti-resonant frequencies (f_a) are different. In order to analyze the effect of the output load on the input impedance, the magnitude and the phase of the input impedance of the transformer was measured for various load resistances, around the operating frequency of the transformer. Fig. 7 shows the resonant and anti-resonant frequencies increase, as load resistance increases. There exists a maximum efficiency, with an optimal load resistance, R_L, of 20 kΩ, which demonstrates a maximum damping ratio in the input impedance, when compared with the other load resistances [27].

In order to investigate the PT, it was simulated using an equivalent circuit, shown in Fig. 8 [3,27]. Using an impedance analyzer (4294A, Agilent, Inc., Palo Alto, CA), the equivalent circuit constants were obtained and calculated as shown in Table 2. In this circuit R, L and C are the equivalent resistance, inductance and capacitance; C_{d1} and C_{d2} are the damped capacitance of the input and output, respectively; n is the transformation ratio of the PT, which is calculated using [28,29]:

$$n = \sqrt{\frac{L_{out}}{L_{in}}} \tag{2}$$

The voltage gain and efficiency are the most important characteristics of a transformer. The two-port networks method was used to analyze the equivalent circuit:

$$\begin{bmatrix} V_{in} \\ I_{in} \end{bmatrix} = \begin{bmatrix} 1 & 0 \\ jwC_{d1} & 1 \end{bmatrix} \begin{bmatrix} 1 & R \\ 0 & 1 \end{bmatrix} \begin{bmatrix} 1 & jwL \\ 0 & 1 \end{bmatrix} \begin{bmatrix} 1 & 1/jwC \\ 0 & 1 \end{bmatrix} \times \begin{bmatrix} 1/n & 0 \\ 0 & n \end{bmatrix} \begin{bmatrix} 1 & 0 \\ jwC_{d2} & 1 \end{bmatrix} \begin{bmatrix} V_{out} \\ I_{out} \end{bmatrix} \tag{3}$$

Eq. (3) can be simplified as follows:

$$\begin{bmatrix} V_{in} \\ I_{in} \end{bmatrix} = \begin{bmatrix} a & b \\ c & d \end{bmatrix} \begin{bmatrix} V_{out} \\ I_{out} \end{bmatrix} \tag{4}$$

Table 2
Parameters of the NKN–01CN piezoelectric transformer equivalent circuit.

	f_r.(kHz)	C_{dl} (pF)	R (Ω)	C (pF)	L (mH)	C_{d2} (pF)	n
PT	223.125	374	15	41	10	30	11.91

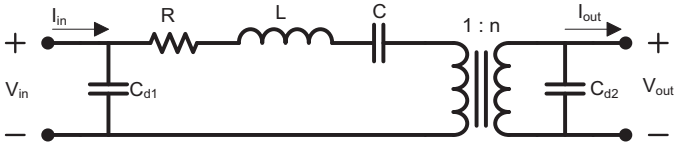

Fig. 8. Equivalent circuit for the input and output of the piezoelectric transformer.

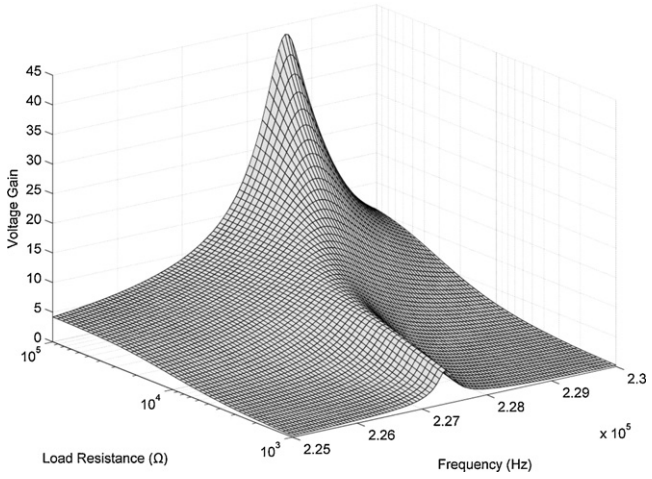

Fig. 9. Simulated voltage gain for various frequencies and load resistances.

Connecting the two-port networks with the load resistance, R_L, the voltage gain (G) and efficiency (η) are

$$G = \frac{V_{out}}{V_{in}} = \left| \frac{R_L}{a \cdot R_L + b} \right| \quad (5)$$

$$\eta = \frac{P_{out}}{P_{in}} = \frac{R_L}{\left|a \cdot R_L + b\right| \cdot \left|c \cdot R_L + d\right| \cdot \cos\ \theta} \quad (6)$$

where θ is the power factor angle. The voltage gain and efficiency, for various frequencies and load resistances, were simulated with MATLAB, using (5) and (6). As shown in Fig. 9, the voltage gain increased from 1 to 43 and the peak frequency slowly changed from 227.4 to 228.5 kHz, when the load resistance was increased from 1 kΩ to 100 kΩ. Fig. 10 shows the simulated efficiency, using (6). The efficiency at peak frequency increased with load resistance; the maximum value was 91.4%, at the optimal load resistance, R_L = 23.3 kΩ. This result is in good agreement with the experimental result shown in Fig. 7.

Fig. 11 shows the experimental results for voltage gain and efficiency, as functions of the load resistance (R_L), measured at V_{in} = 10 V_{rms} (the simulation results is indicated by red lines). For this measurement, the frequencies were adjusted so that the voltage gain and efficiency attained maximums, for the given load resistance. It can be seen that the maximum voltage gain increases with load resistance, with a maximum value of 49, for R_L = 100 kΩ. Fig. 11(b) shows the effect of load resistance on the efficiency of the

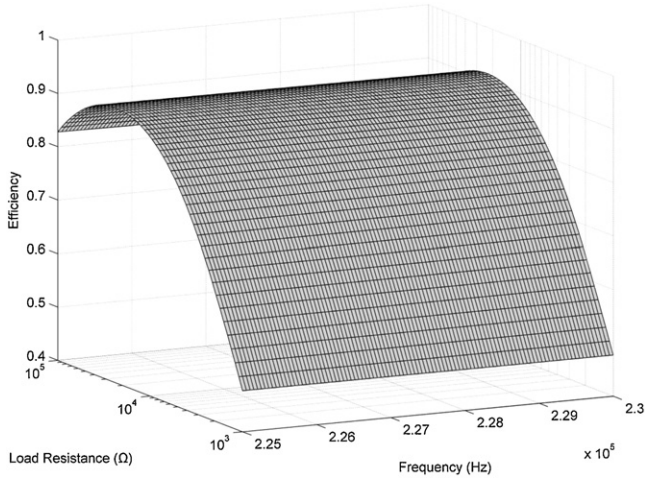

Fig. 10. Simulated efficiency for various frequencies and load resistances.

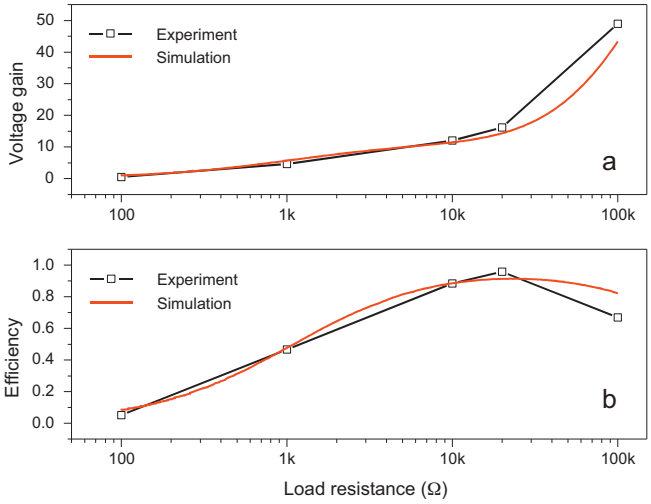

Fig. 11. Experimental and simulation results for (a) voltage gain and (b) efficiency as functions of the load resistance (R_L).

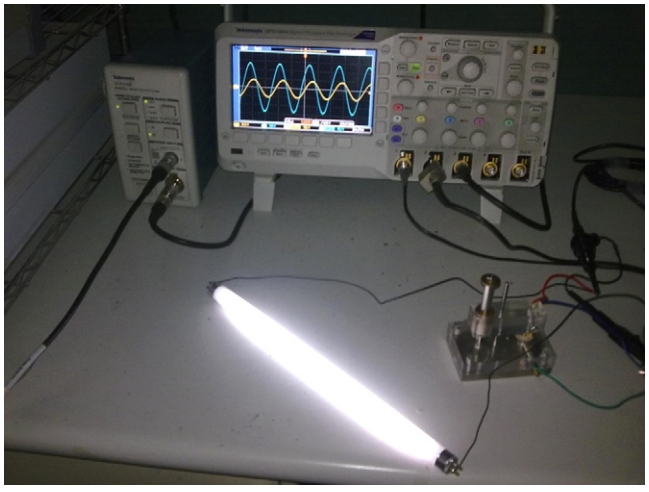

Fig. 12. 8 W T5 fluorescent lamp driven by an NKN–01CN PT.

NKN–01CN PT. A maximum efficiency of 195.7% was obtained, for R_L of 20 kΩ. The experimental results are in good agreement with the simulation results. The maximum efficiency was 91.4%, with voltage gain at R_L = 23.3 kΩ; this is the optimal operating point of the PT.

Table 3 shows a comparison of NKN–01CN and PZT-based (PNW–PMN–PZT) piezoelectric transformers. The ring/dot area ratio is the input electrode area divided by the output electrode area of PTs. The piezoelectric characteristics of PZT-based ceramics are superior to those of NKN–01CN ceramics. These properties influence their use as a piezoelectric transformer. Table 3 lists that the efficiency of PZT-based PT is higher than that of NKN–01CN PT.

Table 3
Comparison of NKN–01CN and PZT-based piezoelectric transformers.

	NKN–01CN	PZT-based
Density, ρ (g/cm^3)	4.47	7.68
Dielectric constant, ε_r	432	1680
k_p (%)	40	52.3
Q_m	1933	1814
Ring/dot area ratio	23.22	1.83
Maximum efficiency (%)	95.7	97.57
Gain (V/V)	14	~1
Reference	Our sample	[6]

The efficiency is the most important property of a PT and PZT-based ceramics with lower impedance yield a higher efficiency. The 8 W T5 fluorescent lamp, lit by the piezoelectric transformer, is shown in Fig. 12; the efficiency was 46%. The efficiency was low, because the resistance of the fluorescent lamp did not match the optimal load resistance of the PT. This problem can be solved by the use of a tracking control system [30].

4. Conclusions

$Na_{0.5}K_{0.5}NbO_3$ + 1 mol% $CuNb_2O_6$ (NKN–01CN) lead-free ceramics with an extraordinarily high mechanical quality factor, Q_m, and density, were prepared using an ordinary ceramic process. The NKN–01CN ceramics exhibit excellent properties, with k_p = 40%, k_t = 45% and k_{33} = 57% and have 'hard' characteristics of E_c = 23 kV/cm and Q_m = 1933. The ceramics also have an excellent temperature coefficient (TCF = −154 ppm/°C), making them suitable for use in lead-free material for piezoelectric transformers. The simulation results were calculated by MATLAB, using an equivalent circuit. These show a maximum efficiency of 91.4%, at a load resistance, R_L = 23.3 kΩ. The experimental results show a maximum efficiency of 95.7% at a load resistance of R_L = 20 kΩ; the experiment results are in good agreement with the simulation results. Simulation with MATLAB allows a prediction of the efficiency, gain and optimum load resistance of the PT and shows these predictions in a 3D model. An 8 W T5 fluorescent lamp was successfully driven using the NKN–01CN PT, but the efficiency was low, because the impedance of the T5 lamp did not match the PT.

Acknowledgements

This work was supported by the National Science Council of Taiwan under grants NSC 97-ET-7-006-005-ET and NSC-98-2112-M-415-001-MY3. The authors would like to thank the Center for Micro/Nano Technology Research, National Cheng Kung University, Taiwan, for providing a single-slide mask aligner.

References

[1] C.A. Rosen, Proceedings of the Electronic Component Symposium, 1956, pp. 205–211.
[2] P. Laoratanakul, A.V. Carazo, P. Bouchilloux, K. Uchino, Jpn. J. Appl. Phys. 41 (2002) 1446–1450.
[3] L. Li, N. Zhang, C. Bai, X. Chu, Z. Gui, J. Mater. Sci. 41 (2006) 155–161.
[4] K.T. Chang, H.C. Chiang, K.S. Lyu, Sens. Actuators A-Phys. 141 (2008) 166–172.
[5] J. Yoo, K. Yoon, S. Hwang, S. Suh, J. Kim, C. Yoo, Sens. Actuators A-Phys. 90 (2001) 132–137.
[6] G. Ivensky, S. Bronstein, S.B. Yaakov, IEEE Trans. Power Electron. 19 (2004) 1446–1453.
[7] X. Chao, Z. Yang, Y. Chang, M. Dong, J. Alloys Compd. 477 (2009) 243–249.
[8] P. Ketsuwan, A. Prasatkhetragarn, N. Triamnuk, C. Huang, A. Ngamjarurojana, S. Ananta, D. Cann, R. Yimnirun, Ferroelectrics 380 (2009) 183–189.
[9] R. Zuo, J. Rodel, R. Chen, L. Li, J. Am. Ceram. Soc. 89 (2006) 2010–2015.
[10] Q. Zhang, B.P. Zhang, H.T. Li, P.P. Shang, J. Alloys Compd. 490 (2010) 260–263.
[11] K.C. Singh, C. Jiten, R. Laishram, O.P. Thakur, D.K. Bhattacharya, J. Alloys Compd. 496 (2010) 717–722.
[12] H.T. Li, B.P. Zhang, P.P. Shang, Y. Fan, Q. Zhang, J. Am. Ceram. Soc. 94 (2011) 628–632.
[13] F. Rubio-Marcos, P. Marchet, X. Vendrell, J.J. Romero, F. Remondiere, L. Mestres, J.F. Ferna, J. Alloys Compd. 509 (2011) 8804–8811.
[14] G. Feng, L. Liangliang, X. Bei, C. Xiao, D. Zhenqi, T. Changsheng, J. Alloys Compd. 509 (2011) 6049–6055.
[15] P.C. Goh, K. Yao, Z. Chen, Appl. Phys. Lett. 99 (2011) 092902.
[16] M. Jiang, X. Li, J. Liu, J. Zhu, X. Zhu, L. Li, Q. Chen, J. Zhu, D. Xiao, J. Alloys Compd. 479 (2009) L18–L21.
[17] M.R. Yang, C.S. Hong, C.C. Tsai, S.Y. Chu, J. Alloys Compd. 488 (2009) 169–173.
[18] R. Huang, Y. Zhao, X. Zhang, Y. Zhao, R. Liu, H. Zhou, J. Am. Ceram. Soc. 93 (2010) 4018–4021.
[19] Y. Zhao, Y. Zhao, R. Huang, R. Liu, H. Zhou, J. Am. Ceram. Soc. 94 (2011) 656–659.
[20] F. Azough, M. Wegrzyn, R. Freer, S. Sharma, D. Hall, J. Eur. Ceram. Soc. 31 (2011) 569–576.
[21] M.R. Yang, C.C. Tsai, C.S. Hong, S.Y. Chu, S.L. Yang, J. Appl. Phys. 108 (2010) 094103.
[22] C.B. Sawyer, C.H. Tower, Phys. Rev. 35 (1930) 269–273.
[23] K. Kakimoto, K. Akao, Y. Guo, H. Ohsato, Jpn. J. Appl. Phys. 44 (2005) 7064–7067.
[24] G. Jiao, H. Fan, L. Liu, W. Wang, Mater. Lett. 61 (2007) 4185–4187.
[27] S.T. Ho, IEEE Trans. Ultrason. Ferroelectr. Freq. Control 54 (2007) 2110–2119.
[28] J. Du, J. Hu, K.J. Tseng, C.S. Kai, G.C. Siong, IEEE Trans. Ultrason. Ferroelectr. Freq. Control 53 (2006) 579–585.
[29] M. Guo, D.M. Lin, K.H. Lam, S. Wang, H.L.W. Chan, X.Z. Zhao, Rev. Sci. Instrum. 78 (2007) 035102.
[30] S. Nakashima, T. Ninomiya, H. Ogasawara, H. Kakehashi, Proc. IEEE APEC'02 1, 2002, pp. 918–924.